

# Maximisation of signal-to-noise ratio in infrared radiation receivers

Z. BIELECKI\*

Institute of Optoelectronics, Military University of Technology, 2 Kaliskiego Str., 00-908 Warsaw, Poland

*The paper describes principles of minimisation of noise produced in infrared detection systems. Analysis of operating conditions affecting signal to noise ratio (S/N) has been carried out. Also analyses for maximisation of S/N in advanced methods of optical signals detection have been made. Many practical solutions have confirmed theoretical predictions.*

**Keywords:** infrared detectors, low-noise preamplifier, thermal imaging systems, non-contact thermometers.

## 1. Introduction

Infrared radiation receivers are used in many up-to-date fields of science and technology determining current level of technological progress. The most important fields of their applications are industrial automation, robotics, space technology, medicine, and military technology.

Three various types of detectors (both thermal and photon ones) are employed in these receivers. The noise produced in detectors and systems of signal conversion constrained detection of low intensity signals (Fig. 1). The works on IR detection are aimed at reduction of detector and preamplifier noise to the value lower than the photon noise one [1,2].

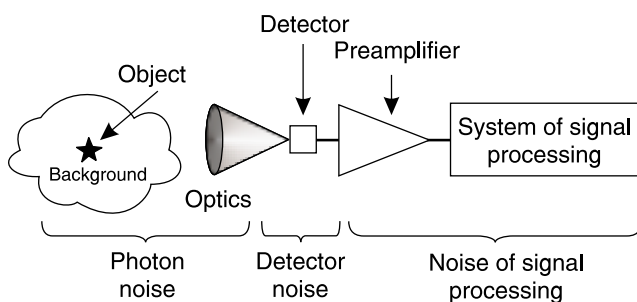


Fig. 1. Noise sources in IR receiver.

To obtain extremely low level of equivalent input noise of a photoreceiver its equivalent scheme should be considered and minimisation of particular noise sources should be done [3].

The literature review showed many works on:

- optimisation of noise of bipolar transistors and field-effect transistors (FET) as well as integrated circuits [4–7],

- technology of IR detectors [1,8–13],
- improvement in IR detector parameters [1,8],
- noise models of photoreceivers used for fibre telecommunication [14–16],
- detector array (hybrid and monolithic one) [17–20],
- signal readout circuits ROICs (readout integrated circuit) [21,22],
- application of IR devices [2,3,23–26].

The work on maximisation of signal-to-noise ( $S/N$ ) ratio was undertaken because of the lack of analyses on selected design parameters and operation conditions of a detector affecting  $S/N$  ratio in direct detection systems and advanced IR methods.

The main purpose was to analyse the input stages of IR receivers and to optimise them providing maximal value of signal-to-noise ratio.

Four main tasks have been done to achieve this aim:

- analyses of noise models of initial stages of IR receivers with consideration of background radiation,
- analyses of  $S/N$  ratio in the receivers with PC and PV detectors,
- optimisation of  $S/N$  ratio in advanced methods of optical signals detection,
- development and performance of the optimised IR receivers.

A general noise model of the input stage of a photoreceiver has been accepted (Fig. 2). Equivalent scheme of a photodetector consists of the signal source, resistance and capacity of a detector, as well as noise sources of a detector and background. As an active element of a preamplifier, bipolar or field-effect transistor (FET) can be used or an integrated circuit with the input at bipolar transistor, FET or metal-oxide semiconductor field-effect transistor (MOSFET). Preamplifier noise is presented as two sources, voltage and current ones. Typical model used for fibre telecommunication does not include a source of background noise. Consideration of such a source is essential in IR receivers used in optoelectronic barriers or laser rangefinders.

\* e-mail: zbiel@wel.wat.waw.pl

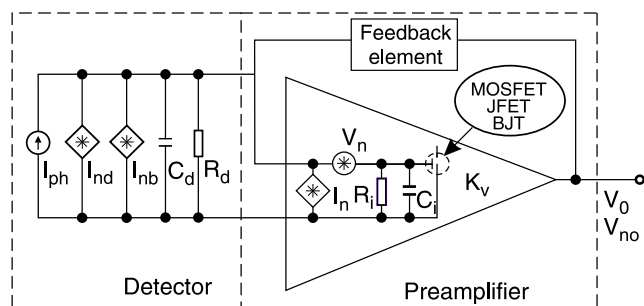


Fig. 2. Equivalent noise model of input stage of photoreceiver (where  $I_{ph}$  is the photocurrent,  $I_{nd}$  is the detector noise,  $I_{nb}$  is the background noise,  $C_d$ ,  $R_d$  are capacity and resistance of a detector respectively,  $I_n$ ,  $V_n$  are current noise and voltage noise of a preamplifier respectively,  $R_i$ ,  $C_i$  are input resistance and input capacity of a preamplifier respectively,  $K_v$  is the voltage gain of a preamplifier).

## 2. Maximisation of signal-to-noise ratio in receivers with photoresistors

Basing on the analysis of noise models of the receivers with photoconductive detectors, the following expression for  $S/N$  ratio can be written

$$\frac{S}{N} = \frac{I_{ph}^2}{\frac{kI_b^a}{f^\beta} + 4q^2\eta(\Phi_s + \Phi_b)Ag^2\Delta f + 4q^2G_{th}g^2\Delta f + \frac{4kT_d\Delta f}{R_d} + \frac{4kT_L\Delta f}{R_L} + I_a^2}, \quad (1)$$

where  $I_{ph}$  is the photocurrent,  $k$  is the Boltzmann constant,  $I_b$  is the bias of the detector,  $f$  is the electrical frequency,  $q$  is the electron charge,  $\eta$  is the quantum efficiency,  $\Phi_s$  is the radiant incident power from the signal,  $\Phi_b$  is the radiant incident power from the background,  $A$  is the detector area,  $g$  is the photoconductive gain,  $\Delta f$  is the electronic frequency bandwidth,  $G_{th}$  is the thermal conductance,  $T_d$  is the detector temperature,  $R_d$  is the detector resistance,  $T_L$  is the load resistance temperature,  $R_L$  is the load resistance, and  $I_a$  is the preamplifier noise.

The numerator exhibits the squared average value of a photocurrent and the dominator shows the total equivalent input noise. The first term of Eq. (1) determines the noise of  $1/f$  type, the second one – generation-recombination noise resulted from fluctuations of radiation from signal and background, the third term – generation-recombination noise produced by thermally excited carriers in semiconductors, next terms represent thermal noise of detector resistance, loading, and preamplifier.

The noise of  $1/f$  type depends on technology of detector manufacturing and the value of a bias current. The second term can be reduced due to narrowing the detector's field of view, application of cooled diaphragms and optical filters. Lowering the detector temperature causes reduction of the third and fourth terms. High load resistance gives ther-

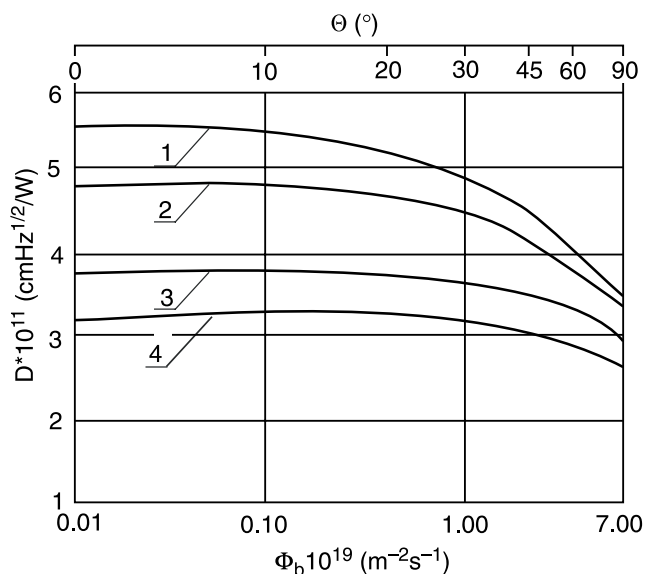


Fig. 3. Detectivity of SPRITE detector vs. angle of field of view. The calculations have been made assuming  $p_0 = 0.9 \times 10^{15} \text{ cm}^{-3}$  (1),  $1.2 \times 10^{15} \text{ cm}^{-3}$  (2),  $1.7 \times 10^{15} \text{ cm}^{-3}$  (3) and  $1.9 \times 10^{15} \text{ cm}^{-3}$  (4).

mal noise minimisation. The optimised preamplifiers of low noise should be used.

Analysis of influence of background radiation on parameters of SPRITE CdHgTe detectors has been made (SPRITE – signal processing in the element). In literature, mainly such detectors operating in the spectral range of 8–14  $\mu\text{m}$  were analysed [27]. Additionally, also SPIRITE detectors of 3–5- $\mu\text{m}$  range were analysed [28]. It results from calculations that for high detector detectivity (i.e., high  $S/N$  ratio), low concentration of equilibrium carriers should be ensured as well as reduction of generation-recombination noise produced by both background radiation and thermally excited carriers (Fig. 3).

## 3. Maximisation of signal-to-noise ratio in receivers with photodiodes

Relation between  $S/N$  ratio and the multiplication factor  $M$  and the material coefficient  $x$  is given in literature. The coefficient  $x$  depends on material of which an avalanche photodiode is made. The values of the coefficient  $x$  are within 0.3–0.5 for a silicon avalanche photodiode and 0.7–1.0 for an avalanche photodiode made of germanium or III-V compounds. To the analysis of  $S/N$  ratio, the influence of temperature was added and then the following expression for  $S/N$  ratio was obtained [29]

$$\frac{S}{N} = \frac{M^2(V,T)I_{ph}^2}{2q\Delta f[(I_{ph} + I_b)M^2(V,T)F[M(V,T)] + (I_s + I_{db}M^2(V,T)F[M(V,T)])2^{(T-100)/10}] + \frac{4kT\Delta f}{R_L}F_n} \quad (2)$$

where  $M$  is the multiplication factor,  $F$  is the photodiode multiplication factor,  $V$  is the bias voltage of the photodiode, and  $F_n$  is the noise factor of the preamplifier.

The numerator includes squared average value of photocurrent multiplied by squared multiplication factor of an avalanche photodiode. Denominator represents the total substitute input noise of a receiver. The first term of Eq. (2) describes shot noise, the second one – thermal noise of load resistance and preamplifier noise. Shot noise depends on

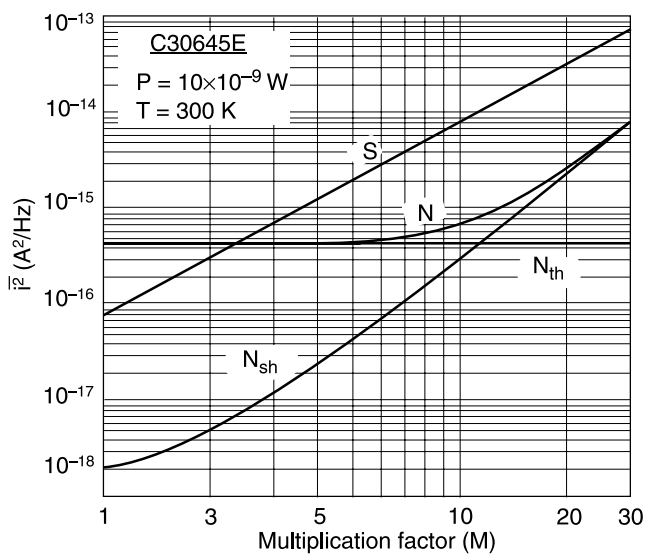


Fig. 4. Dependence of signal, shot noise, thermal and total noises on the avalanche multiplication factor  $M$ .

photocurrent, background current, as well as on superficial and volumetric components of dark current.

The diagram below has been drawn on the basis of numerical calculations. It presents dependence of signal, shot noise, thermal and total noise on the avalanche multiplication factor  $M$  (Fig. 4).

For low values of the factor  $M$ , the signal amplitude is lower than the noise amplitude. With the higher factor  $M$ , both the signal and the noise increase. There is exactly determined value of the avalanche multiplication factor  $M$  for which the distance between a straight line representing a signal and a curve representing the total noise is the longest one. It corresponds to the case when  $S/N$  has its maximum value. For the given photodiode and temperature, the value of bias voltage is exactly determined, for which  $S/N$  has its maximum [29].

These analyses have been verified experimentally and special supply module has been designed (Fig. 5). This module ensures APD operation with maximum value of  $S/N$  ratio in wide range of temperature changes and it was applied in a receiver for laser rangefinder with a source of eye-safe radiation.

The investigation results show that for high value of  $S/N$  in the receivers with photovoltaic detectors the following activities should be done:

- minimisation of the noise from background, detector, bias circuit and preamplifier,
- lowering temperature of detector operation,
- selection of optimal working point of APD by using low-noise supply modules.

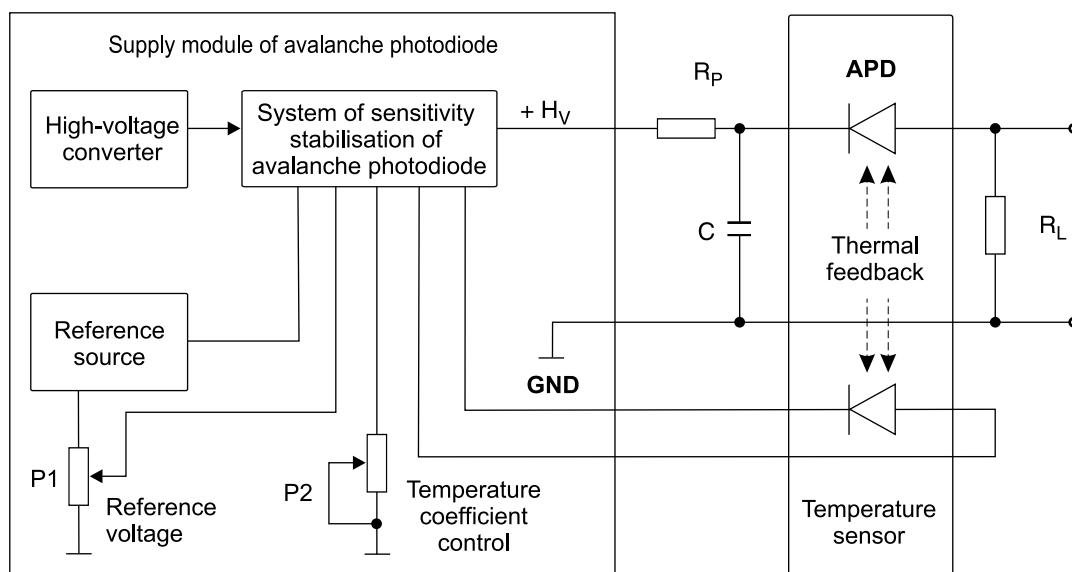


Fig. 5. Supply system of avalanche photodiode ensuring maximum value of  $S/N$  ratio with ambient temperature changes.

#### 4. Maximisation of signal-to-noise ratio in advanced methods of optical signals detection

Improvement in  $S/N$  ratio has been done in the following systems:

- detection system with averaging of measurement results,
- phase-sensitive detection system,
- detection system with synchronic integration of a signal.

In the systems of IR detection with integrated circuit (Fig. 6),  $S/N$  ratio is directly proportional to the integration time

$$\frac{S}{N} = \frac{2v^2 t}{S_n}, \quad (3)$$

where  $v$  is the voltage at the input of the integrated circuit,  $t$  is the integration time, and  $S_n$  is the spectral density of noise power.

The integration process in mathematical sense means summation of measurements. If we make  $m$  measurement, each integrated over a period,  $t$ , and add them we obtain a result whose signal-to-noise ratio is

$$\frac{S}{N} = \frac{2v^2 mt}{S_n}. \quad (4)$$

Note, that choice of the value of integration time constant, does not affect the  $S/N$  ratio.

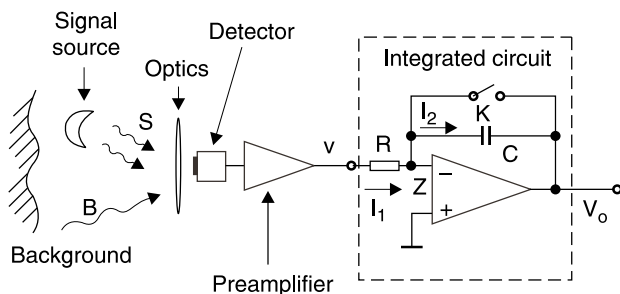


Fig. 6. Scheme of signal detection system with analogue integrator.

In a real measurement, we should simply choose the value of integration time constant which provides a convenient output level after each sample integration period. When the signal is measured in the presence of white noise we get a final  $S/N$  power ratio, which improves, proportionally to the measurement time (i.e. the  $S/N$  voltage ratio increases with the square root of the time of measurement).

New system of phase-sensitive detection with reduction of background radiation has been elaborated (Fig. 7). The phase-sensitive detection method is widely used in the systems with  $1/f$  noise and unwanted background levels. This system differs from commonly used phase sensitive detector (PSD) system because here the additional radiation source  $S_2$  is applied, i.e., the mirror with a special modulating plate. We used a reflecting chopper made of a shiny

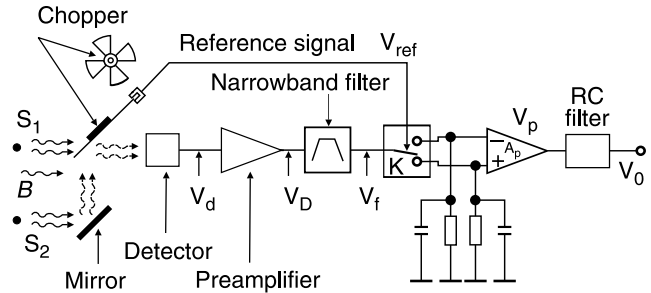


Fig. 7. Scheme of PSD detection system for reduction of constant component or slowly varying one resulting from background radiation.

material. When its blades block the signal, the detector will see the light reflected from the chopper surface.

If we define  $S_1$ ,  $S_2$ , and  $B$  to be the power levels produced by the two sources and the background, a detector whose responsivity is  $R_v$  will produce an output voltage

$$V_1 = R_v(S_1 + B), \quad (5)$$

when the signal path to  $S_1$  is clear, and the voltage

$$V_2 = R_v(S_2 + B), \quad (6)$$

when one of the reflecting blades fills the detector's field of view.

The amplitude  $V$  of the alternating signal at the detector output is

$$V = V_1 - V_2 = R_v(S_1 + S_2) \quad (7)$$

In a typical PSD system, the voltage at the measuring system output includes a component of background radiation. The peak-to-peak value of the voltage at the detector output does not include this component.

The systems for phase-sensitive detection are used for measurement of constant-intensity signals or slowly varying ones. In many cases it is necessary to measure periodic pulse signals of very low amplitudes, even the signals of amplitude below the level noise value. For such cases, the detection systems with synchronic signal integration are used. A scheme of such a system is shown in Fig. 8.

The technique can be employed in various ways provided two basic requirements are obeyed. Firstly, the signal must be repeatable so, we can produce a series of nominally identical pulses. Secondly, we must obtain an extra trigger signal-similar to the phase reference signal required for a PSD.

Increase in  $S/N$  ratio is obtained for larger number of measuring cycles  $m$  and longer time  $t_m$  of key switching on

$$\frac{S}{N} = V_D(t)m \left( \frac{2t_m}{S_n} \right), \quad (8)$$

where  $V_D(t)$  is the voltage at the preamplifier output.

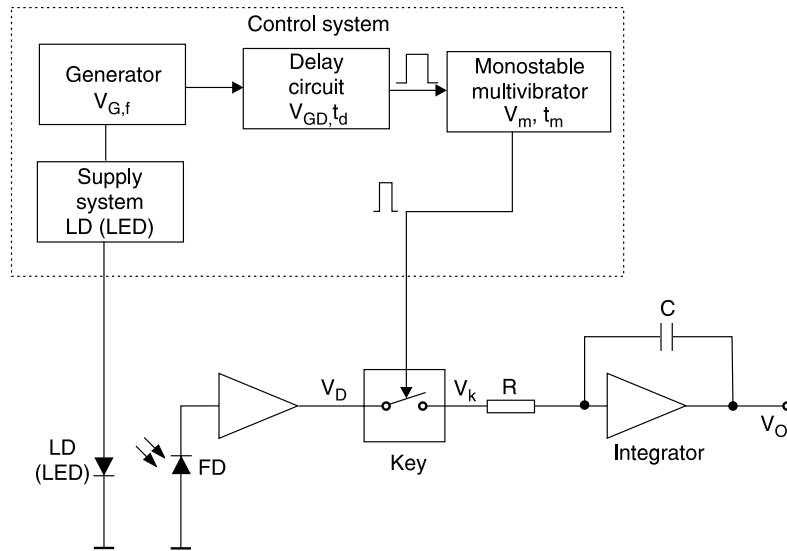


Fig. 8. Detection system with synchronic integration of a signal.

Hence, when we improve the  $S/N$  ratio by increasing  $m$ , the measurement takes longer. A drawback of the method considered so far is the fact that for most of the time the output integrator is disconnected from the input. Only the fraction of the pulses  $t_m/T$ , while the key is closed, contribute to the measurement result. As a consequence, to measure all the details of the pulse shape we have to repeat the measurement process up to  $T/t_m$  times for each value (where  $T$  is the period time and  $t_d$  is the delay time).

### 5. Applications

This section describes exemplary devices designed and performed at the Institute of Optoelectronic MUT. These devices employ optimised receivers of infrared radiation.

One of them is a photoreceiver for laser rangefinder with an IR source operating in eye-safe range (Fig. 9). This receiver includes earlier described system of polarisation

and stabilisation of avalanche multiplication factor of APD. It allows us to detect laser pulses of duration 100 ns and power below 10 nW [30].

The other device is a multispectral IR pyrometer used for remote temperature measurements [31,32]. The multi-band pyrometer was developed for non-contact temperature measurement of the objects with unknown and wavelength-dependent emissivity. The pyrometer was designed using single thermoelectrically cooled PbS detector of spectral band of 1–2.5  $\mu\text{m}$  and 8 narrow-band filters. Temperature measurements are possible of the objects at temperature within the range of 500°C–1200°C and frequency 75 Hz. It can be used for controlling various industrial-technological processes as well as in research works for testing typical singleband pyrometers and temperature measurement of the objects the emissivity of which depends on wavelength and time.

In order to have maximum value of  $S/N$  ratio the following activities have been performed:

- selection of optimal current supplying PbS detector,

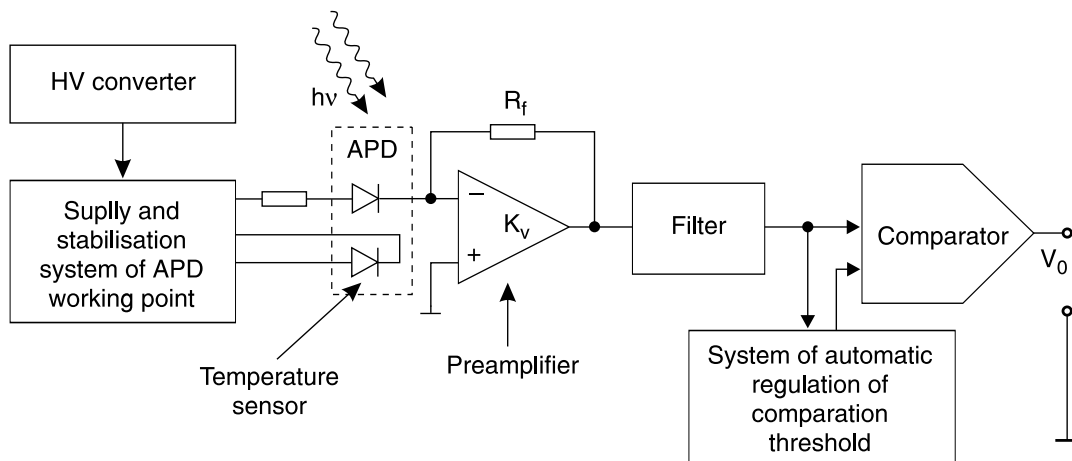


Fig. 9. Block diagram of a photoreceiver for laser rangefinder operating within the eye-safe range.

- lowering operation temperature of a detector using thermoelectric cooler (TEC),
- application of optimised signal preamplifier,
- selection of optimal rotation frequency of a plate on which eight optical filters are fitted. (Fig. 10).

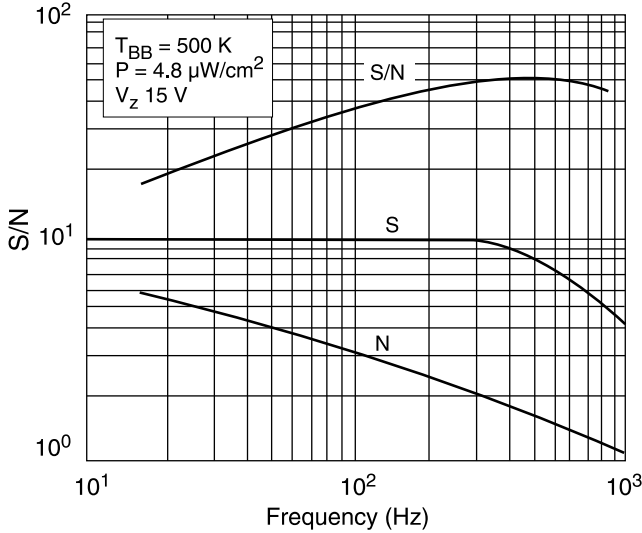


Fig. 10. Dependence of signal, noise, and S/N ratio on frequency of plate.

Original device is a laboratory model of passive locator of flying objects (Fig. 11). It consists of the system of image scanning, thermodetection head, control, and data acquisition and visualisation modules.

The device scans a  $360^\circ \times 20^\circ$  sector in 1 second. Accuracy of location of the detected object is equal to  $\pm 1^\circ$ . The scanner (Fig. 11) consists of a single mirror, which rotates horizontally with high speed and simultaneously swings vertically. Stabilised rotation is driven by DC motor, while swing is due to stepping motor and worm gear.

The device can work with two replaceable thermodetection modules consisting of silicon-germanium focusing objective, a detector with thermoelectric cooler and optimised low-noise preamplifier. This device includes two exchangeable thermodetection modules (with PV and

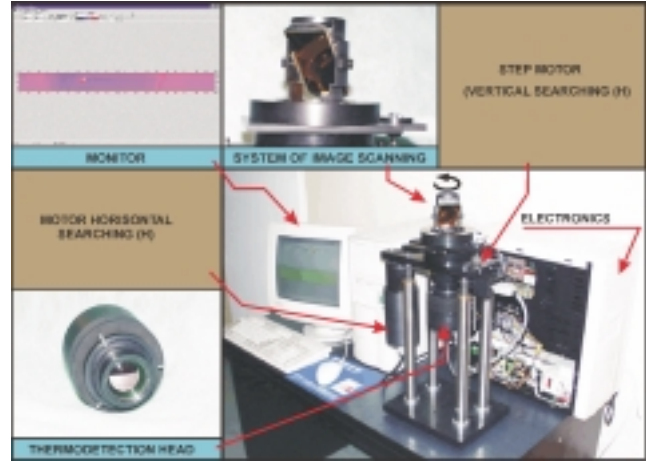


Fig. 11. Photo of a device.

PC detectors) optimised for the spectral range of 3–4.2  $\mu\text{m}$ .

Data acquisition, preliminary processing and visualisation is performed by PC with graphic card and PCL-816 Data Acquisition Card (Advantech). Special software working on the Windows 95/98 platform and using Advantech DLL libraries was designed.

In some receivers with pyroelectric detectors popcorn noise is produced. Such noise at the output of a detection system is received as a signal from short existing thermal object, which can be a source of false alarm. Figure 12 shows the block diagram of the microprocessor circuit for the detector [33,34]. There are nine main blocks: preamplifier, filter, A/D converter, digital signal processor, D/A converter, low frequency filter, data memory, and program memory. Signal from the preamplifier and low pass filter is converted into a 16 bit A/D converter. In the digital signal processor circuit (DSP), a spectrum of the signal is compared with mathematical model of the popcorn noise. If the popcorn noise is produced, its spectrum is removed by the digital filter in the DSP. Then, inverse fast Fourier transform was applied to the signal. So, we can remove a spectrum of the popcorn noise. At the output, only the signal from a thermal object is received.

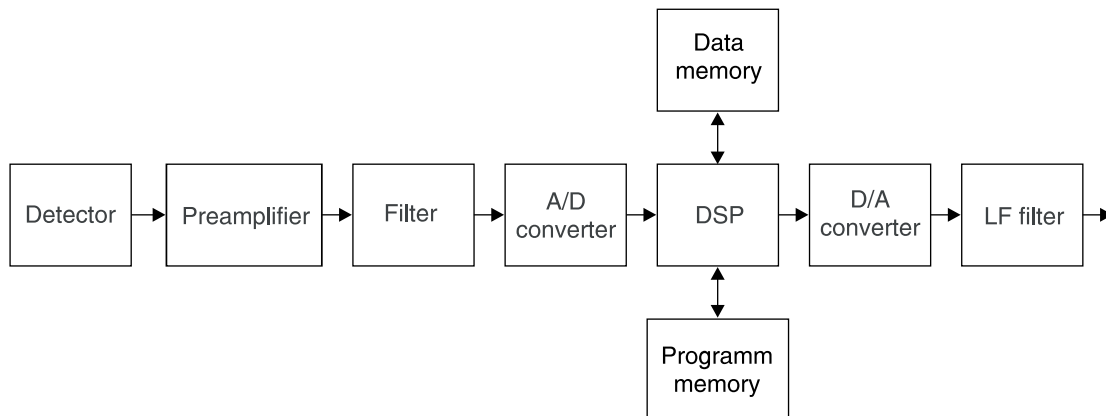


Fig. 12. Block diagram of a new receiver for pyroelectric detector.

Table 1. Parameters of infrared detectors.

Preamplifier for detector	Amplification	Band [kHz]	Noise current [ $\text{fA}/\text{Hz}^{1/2}$ ]	Voltage current [ $\text{nV}/\text{Hz}^{1/2}$ ]	Type of input elements
Si Photodiode	$1.35 \times 10^8$ V/A	0.01–85	0.6	11	TLC 2201
Ge Photodiode	$1.35 \times 10^8$ V/A	0.01–85	140	10	OP 07
InGaAs Photodiode	44 dB	DC–30 MHz	2000	2.5	AD 8001
PbS/PbSe Photoresistor	60 dB	0.08–250	$1000/R_d^*$	11	TLC 2201
PbS – TEC Photoresistor	$2.7 \times 10^8$ V/A	0.01–65	0.6	11	TLC 2201
$R_d = (50\text{--}500) \Omega$ Photoresistor	$4.7 \times 10^8$ V/A	0.01–65	0.6	11	TLC 2201
$R_d = (50\text{--}500) \Omega$ Photoresistor	$10^5$ V/A	0.007–100	$1000/R_d^*$	1	2SD 786
$R_d = (50\text{--}500) \Omega$ Photodiode	$10^4$ V/A	0.01–100	$1000/R_d^*$	1	LT 1028
$R_d = (50\text{--}500) \Omega$ Photodiode	$4 \times 10^6$ V/A	0.008–400	$4000/R_d^*$	4	2N 4393

\*  $R_d$  value in  $\text{k}\Omega$

Also low-noise preamplifiers for various types of IR detectors were elaborated. The obtained parameters are presented in Table 1.

An idea of synchronic receiving was applied in optoelectronic base sensor (Fig. 13). The sensor contains a transmitter (system of control logic and laser controller) and a photoreceiver (input stage of the photoreceiver, detector of a peak value, comparator, and counter). The detector of a peak value is used to define maximal received pulse. A loop connecting control system with the receiver counter checks compatibility of the received pulses with the pulses from a control generator. At the moment when the received signal is of maximal value, the pulse is generated initiating a bomb detonator. Such sensors can be applied in aerial bombs to destroy stationary targets, e.g., airports, road, and the like.

## 6. Conclusions

New detection systems, with better  $S/N$  ratio than hitherto known ones, were theoretically analysed. Development of these systems included:

- comparison of direct detection systems and advanced methods of IR detection for  $S/N$  ratio estimation,
- classification of substitute noise schemes of the input stages of photoreceivers with photoconductive and photovoltaic detectors,
- determination of operation conditions of the input stages of photoreceivers the noise level of which is close to the noise determined by fluctuation of a number of photons incident on a detector,
- analysis of background radiation influence on detectivity of SPRITE detectors (3–5  $\mu\text{m}$ ),

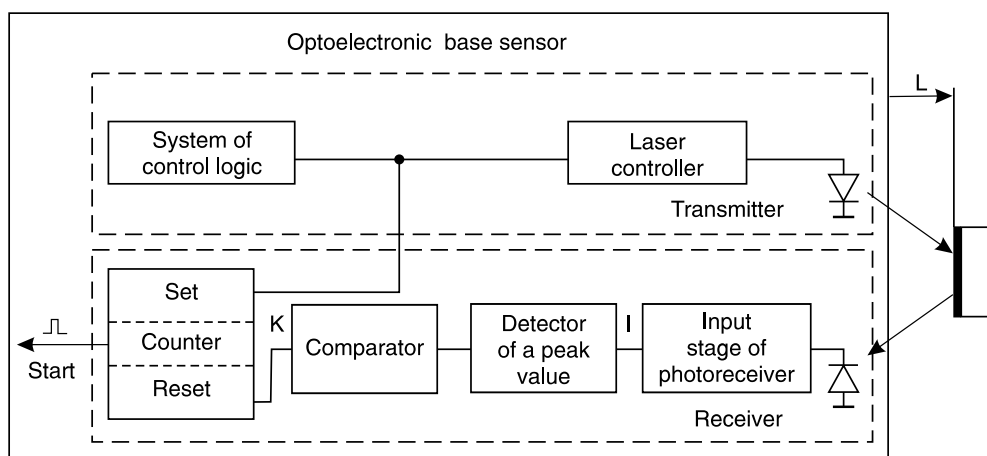


Fig. 13. Block diagram of contactless optoelectronic distance-sensor of a base type.

- computer simulation of receivers with APD and analysis of supply systems for maximum  $S/N$  ratio in wide range of temperatures,
- development of a system eliminating free fluctuations of background radiation,
- analysis of  $S/N$  ratio in advanced methods of optical signals detection.

The results of the above mentioned activities were used for experimental investigations, i.e., several IR detection devices were designed, performed, and tested. The results presented in this work do not comprise all the problems of optimisation of  $S/N$  ratio in IR receivers. However, it includes complete analysis of direct detection systems and description of advanced methods of IR signals detection. The carried out analyses and experimental investigations can be used also for detection of UV signals.

## References

1. A. Rogalski and J. Piotrowski, "Intrinsic infrared photo-detectors," *Prog. in Quant. Electr.* **12**, 87–289, (1988).
2. G.H. Rieke, *Detection of Light: from the Ultraviolet to the Submillimeter*, Cambridge, Cambridge University Press, 1994.
3. E.L. Dereniak and G.D. Boreman, *Infrared Detectors and Systems*, New York, Wiley, 1996.
4. C.D. Motchenbacher and J.A. Connelly, *Low-noise Electronic System Design*, New York, Wiley, 1995.
5. J.L. Vampola, "Readout electronics for infrared sensors," in *The Infrared and Electro-Optical Systems Handbook*, Vol. 3, edited by W.D. Rogatto SPIE Press, Bellingham, 1993.
6. Z. Bielecki, "Low noise electronics for IR detectors," *Proc. IRS<sup>2</sup>*, 135–138 (2000).
7. Z. Bielecki, "Optimisation of signal detection systems operating with various IR detectors," *6<sup>th</sup> Topical Meeting on Education and Training on Optics and Photonics, ETOP'99 P (III) -19*, Cancun, Mexico, 40 (1999).
8. A. Rogalski, *Infrared Detectors*, Amsterdam, Gordon and Breach Science Publishers, 2000.
9. J.S. Ascetta and D.L. Shumaker, *The Infrared and Electro-Optical Systems Handbook*, Vol. 4, SPIE Optical Engineering Press, Bellingham, 1993.
10. E.H. Putley, "Thermal detectors," in *Optical and Infrared Detectors*, pp. 71–100, edited by R.J. Keyes, Springer, Berlin, 1977.
11. R.F. Dillon, D.P. DeGloria, F.M. Paglighi, J.T. Muller, M.G. Cheifetz, D.E.B. Lees, and M. Michalik, "Low-cost laser radar imaging experiments," *SPIE* **1633**, 274–280 (1992).
12. A. Rogalski, *Infrared Photon Detectors*, SPIE Optical Engineering Press, Bellingham, 1995.
13. J. Piotrowski, "Breakthrough in infrared technology – the micro-machined thermal detector arrays", *Opto-Electron. Rev.* **3**, 3–8 (1995).
14. G. Keiser, *Optical Fibre Communications*, McGraw-Hill, New York, 1979.
15. W.K. Pratt, *Laser Communication Systems*, Wiley, New York, 1969.
16. H. Kressel, "Semiconductor devices for optical communication," *Topics in Applied Physics* **39**, New York, 1980.
17. L.J. Kozlowski and W.F. Kosonocky, "Infrared detector arrays," in *Handbook of Optics*, Chap. 23, edited by M. Bass, E.W. Van Stryland, D.R. Williams, and W.L. Wolfe, McGraw-Hill, Inc. New York (1995).
18. L.J. Kozlowski, S.A. Cabelli, D.E. Cooper, and K. Vural, "Low background infrared hybrid focal plane array characterisation," *SPIE* **1946**, 199–213 (1993).
19. L.J. Kozlowski, K. Vural, J. Luo, A. Tomasini, T. Liu, and W.E. Kleinhans, "Low-noise infrared and visible focal plane arrays," *Opto-Electron. Rev.* **7**, 259–269 (1999).
20. L.J. Kozlowski, R.B. Bailey, S.C. Cabelli, D.E. Cooper, G. McComas, K. Vural, and W.E. Tennant, "640×640 PACE HgCdTe FPA," *Proc. SPIE* **1735**, 163–174 (1992).
21. D.A. Scribner, M.R. Kruer, and J.M. Killiany, "Infrared focal plane array technology," *Proc. IEEE* **79**, 66–85 (1991).
22. L.J. Kozlowski, J.M. Arias, G.M. Williams, K. Vural, D.E. Cooper, S.A. Cabelli, and C. Bruce, "Recent advances in staring hybrid focal plane arrays: comparison of HgCdTe, InGaAs, and GaAs/AlGaAs detector technologies," *Proc. SPIE* **2274**, 93–116 (1994).
23. J.D. Vincent, *Fundamentals of Infrared Detector. Operation and Testing*, Wiley, New York, 1990.
24. M.I. Skolnik, *Radar Handbook*, New York, Mc. Graw-Hill Comp., 1990.
25. G. Gaussorgues, *La Thermographie Infrarouge*, Lavoise, Paris, 1984.
26. M.C. Dudzik, "Electro-optical systems design, analysis, and testing," in *The Infrared and Electro-Optical Systems Handbook*, Vol. 4, pp. 299–342, SPIE Optical Engineering Press, Bellingham, 1993.
27. C.T. Elliot, D. Day, and D.J. Wilson, "An integrating detector for serial scan thermal imaging," *Infrared Phys.* **22**, 31–42 (1982).
28. Z. Bielecki, "Influence of background radiation on performance of SPRITE detectors," *Proc. SPIE* **2321**, 242–245 (1994).
29. Z. Bielecki, "Analysis of operation conditions of avalanche photodiode on signal to noise ratio," *Opto-Electron. Rev.* **5**, 249–256 (1997).
30. Z. Bielecki. "Photoreceiver with avalanche C-30645 photodiode" *IEE Proceedings Optoelectronics*, **147**, 234–236 (2000).
31. Z. Bielecki, K. Chrzanowski, R. Matyszkiewski, T. Piątkowski, and M. Szulim, "Infrared pyrometer for temperature measurement of objects of both wavelength and time dependent emissivity", *Optica Appl.* **29**, 285–292 (1999).
32. Z. Bielecki, K. Chrzanowski, R. Matyszkiewski, T. Piątkowski, and M. Szulim, "Infrared pyrometer for temperature measurement of objects, emissivity of which depends on wavelength and time", *Quantitative Infrared Thermography 4*, "Proc. Eurotherm Seminar," 316–321 (1998).
33. Z. Bielecki, "Photoreceiver with popcorn-noise reduction systems," *26<sup>th</sup> International Conference on Infrared and Millimeter Waves*, 10–14 September, Toulouse, France, 72–73 (2001).
34. Z. Bielecki, "Elimination of popcorn noise in receivers with pyroelectric detectors". International Conference Infrared Sensors & Systems, Erfurt, *Proc. IRS<sup>2</sup>*, 173–177 (2002).